Strength and stiffness of silty clay with variable saturation

T. Mohyla, J. Jerman, J. Rott, J. Boháč & D. Mašín
Charles University, Faculty of Science, Department of Engineering Geology, Prague

ABSTRACT: The strength and stiffness of a silty soil in dependence of its saturation were tested using conventional and advanced triaxial devices. The tested soil was a low plasticity silty clay from Central Bohemia. Reconstituted and compacted specimens were tested. The tests on unsaturated soil were controlled using the concept of net stress and suction. The experiments were aimed at determining parameters for a hypoplastic constitutive model for unsaturated soils and therefore the processing of data and the calibrations used the effective stress concept. In processing the strength data obtained by unconfined compression tests the capillary cohesion concept, and the linear form of extended Mohr – Coulomb strength envelope were adopted. The results confirmed the good performance of the advanced constitutive model, and also showed the applicability of the capillary cohesion and suction stress concept for the strength testing and interpretation.

1 INTRODUCTION

The strength and stiffness of an unsaturated low plasticity clayey soil were tested using both conventional and advanced triaxial devices. The tests were controlled using the concept of two independent stress variables, namely net stress and suction (Fredlund and Morgenstern, 1977). Since the experiments were aimed at determining parameters for the hypoplastic constitutive model for unsaturated soils (Wong and Mašín, 2014), in processing the data and in the calibrations the effective stress concept was adopted (Bishop, 1959), with the effective stress parameter χ due to Khalili and Khabbaz (1998).

In studying the very-small and small strain stiffness the concept of current suction ratio (CSR) and recent suction history proposed by Ng and Xu (2012) was adopted. The definition of their concept is in Figure 1.

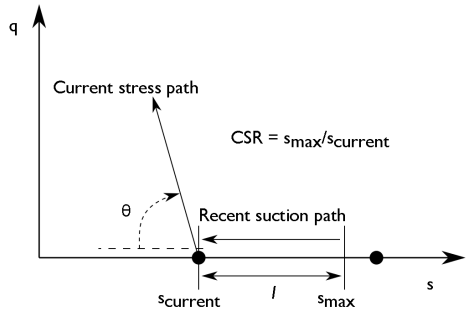

Figure 1. CSR and recent suction history; adapted from Ng and Xu (2012).

The conventional triaxial CIUP strength tests on reconstituted specimens were carried out to determine the critical state strength. Further, simple unconfined compression tests on compacted specimens with different water contents were performed with the aim to estimate the suction and undrained strength in the soil subjected to standard laboratory compaction (Standard Proctor compaction effort). In processing the strength data obtained by unconfined compression tests the capillary cohesion concept, and the linear form of extended Mohr – Coulomb strength envelope were used (e.g., Fredlund et al., 2012; Lu and Likos, 2004).

2 A SIMPLIFIED CONCEPT OF STRENGTH OF SOIL AT CONSTANT WATER CONTENT

The undrained strength of a water saturated fine grained soil can be quantified using the state boundary surface (Schofield and Wroth, 1968). The concept is also applied in the hypoplastic model. Therefore the undrained strength s_u can be directly related to the current void ratio or equivalently to the current Hvorslev's equivalent pressure. Alternatively, the undrained strength can be estimated from liquidity/consistency index (Sharma and Bora, 2003; Herle et al., 2011).

In the unsaturated state with constant water content, the short-term stability is not fully undrained. However, when suction is lower than the air-entry value, the soil is near to the saturated state (the fu-

nicular regime), water phase is continuous, and the pressure of the air phase approximately corresponds to the pressure of the water (strictly it is slightly higher due to the surface tension of water). In a simplified analysis, when the soil is in the funicular state, saturated undrained strength can be adopted for calculation of slope stability. The undrained strength will be determined from the state boundary concept, irrespective of the value of suction.

When suction is higher than the air-entry value, the pressure of the pore air can be assumed to correspond to the atmospheric pressure, the air-phase being continuous. The effective stress (Khalili and Khabbaz, 1998) can be adopted for the unsaturated soil, and assuming the relevance of critical state strength the simple strength envelope of Figure 2 is applicable.

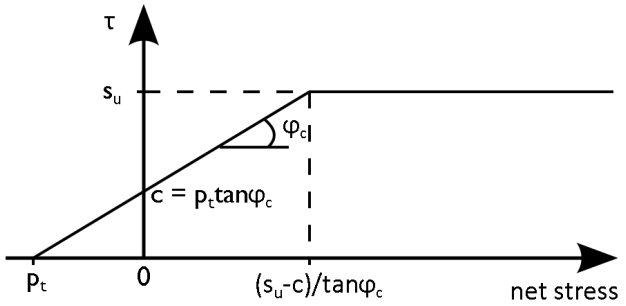

Figure 2. Concept of strength envelope for unsaturated soil at constant water content.

From known water content and voids ratio the shift of the failure envelope by p_t can be computed ($p_t = s\chi$; s is capillary suction). The apparent cohesion c can be used in stability analyses. If the water content varies with the depth the analysis is carried out independently in each depth.

Figure 2 shows that the undrained strength of unsaturated soil ('quick loading') is lower than the undrained strength of the same soil at the same water content when saturated. On the other hand, in drained ('slow') loading, when the water content changes, the unsaturated soil is stronger than the saturated soil.

3 THE TESTED SOIL

The tested soil was loess from Central Bohemia. The soil has the liquid limit and plasticity index of 29 and 11, respectively. The description and the basic properties of the soil are summarized in Table 1.

4 SPECIMEN, TESTING PROCEDURE

4.1 *Strength - triaxial CIUP tests*

The critical state strength of the tested soil was determined in conventional CIUP triaxial tests on reconstituted specimens with the diameter of 38 mm and the height of ca 76 mm. For reconstituting, the grains larger than 0.5 mm were removed. The slurry with the water content above the liquid limit was consolidated in a high press of the diameter equal to triaxial specimens, i.e. 38 mm, with the vertical stress of 100 kPa. After extruding from the press, the length was cut to about 76 mm.

Table 1. Basic properties of the loess.

Property	
Standard compaction tests	
Maximum dry density (kg/m^3)	1810
Optimum moisture content (%)	15
Grain size distribution	
Sand content (≤ 2 mm, %)	22
Silt content (≤ 63 μm, %)	68
Clay content (≤ 2 μm, %)	10
Specific gravity	2.71
Atterberg limits	
Plastic limit (%)	18
Liquid limit (%)	29
Plasticity index (%)	11
Unified soil classification system (USCS)	CL

Further to the critical state strength the estimates of undrained strength s_u based on the concept of critical states (CSSM) and/or on hypoplastic model were checked by a pilot CIUP test on a compacted specimen saturated prior to triaxial testing at its effective stress due to standard compaction effort (Standard Proctor). During saturating the effective stress corresponding to the estimated effective stress in the compacted soil (Bishop's stress with $\chi \approx S_r$) was applied. After saturating, it was checked whether the dimensions have not changed, i.e., whether the principle of effective stress was observed, and the specimen was subjected to a conventional CIUP test.

4.2 *Strength – unconfined compression tests*

Standard triaxial specimens of 38 mm in diameter and twice the height were prepared from the compacted samples of about 110 mm diameter using the conventional hand-operated specimen lathe. The compacted samples were prepared according to Standard Proctor test with different water contents of 9, 11, 14 and 17%. The specimens were sheared at the constant axial deformation rate of 1.5 mm/min.

4.3 *Stiffness – triaxial tests*

The stiffness measurements were carried out in the double walled triaxial cell. The specimens were reconstituted in the same way as for the critical state strength testing. Suction was introduced to the initially saturated specimens after their setting up in the triaxial cell, using conventional flow pumps (GDS or VJT volume/pressure controllers). The double walled triaxial cell was equipped with the high air

entry disk (500 kPa) and a standard porous stone at the bottom and top end of the specimen, respectively. The applied stress paths are shown in Figure 3.

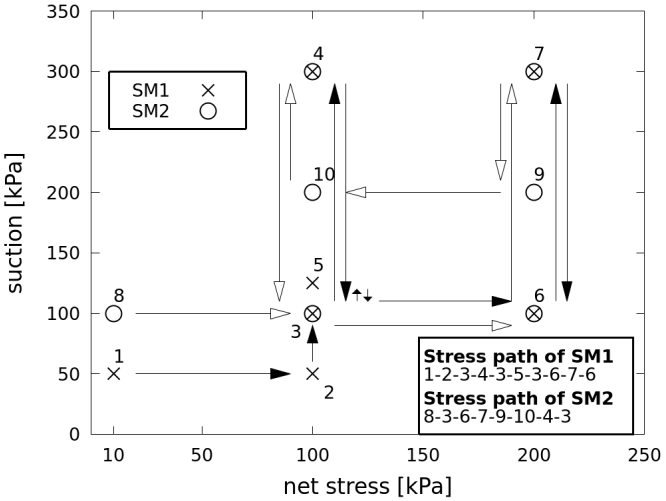

Figure 3. Stress paths (suction vs net stress) applied in studying stiffness of the reconstituted soil.

At each equalization stage, the maximum shear stiffness was measured by bender elements. Then a small drained shear probe of the conventional compression stress path (σ_r = *const.*) and with the maximum deviator stress change of 30 kPa was carried out, with local axial deformation measurements (submersible LVDTs).

Two specimens were tested but the stiffness decay curve was measured with the second one only (SM2). The test procedure of the specimen SM2 is summarized in Table 2. The identification of the measurements in Table 2 is defined as follows: P is the current net stress, S is the current suction, C is the current suction ratio and L is the magnitude of the recent suction change.

Table 2. Test stress states and their history for measuring the stiffness of specimen SM2.

Test ID	Stress path
SM2_P10S100C1L100	0-8
SM2_P100S100C1L0	8-3
SM2_P200S100C1L0	8-3-6
SM2_P200S300C1L200	8-3-6-7
SM2_P200S200C1.5L100	8-3-6-7-9
SM2_P100S200C1.5L0	8-3-6-7-9-10
SM2_P100S300C1L100	8-3-6-7-9-10-4
SM2_P100S100C3L200	8-3-6-7-9-10-4-3

5 CONSTITUTIVE MODEL

5.1 *Model description*

The model used in this study is coupled hydro-mechanical hypoplastic model for unsaturated soils. It incorporates the small strain stiffness, which is predicted with respect to the intergranular strain concept proposed by Niemunis and Herle (1997), but modified for the unsaturated conditions. The model is capable of reproducing both recent suction and stress histories.

The maximum shear modulus is calculated by the following equation:

$$G_0 = p_r A_g \left(\frac{p}{p_r}\right)^{n_g} e^{-m_g} \left(\frac{s}{s_e}\right)^{k_g} \quad (1)$$

where is p_r reference pressure of 1 kPa; A_g, n_g, m_g and k_g are parameters controlling the dependency of G_0 on mean effective stress, void ratio and degree of saturation.

For detailed description of the model see the paper by Wong and Mašín (2014).

6 RESULTS

6.1 *Critical state strength*

Conventional triaxial CIUP tests on reconstituted specimens were carried out in determining the CSL of the soil: $\varphi_{cr} = 30°$; $\Gamma = 1.234$; $\lambda = 0.1234$; $C_c = 0.2840$ (Figures 4 and 5).

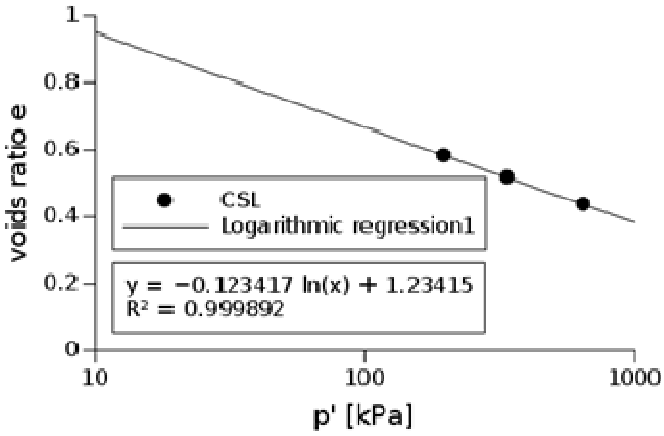

Figure 4. CSL of the tested soil in the plane e vs p'.

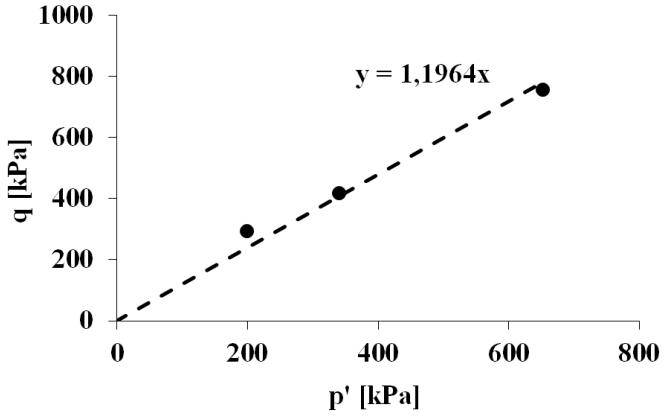

Figure 5. CSL of the tested soil in the plane q vs p'.

6.2 *Unconfined compression strength*

Interpretation of tests on compacted specimens has been based on the assumption that their shear behaviour is controlled by the critical state friction angle,

that the original structure of the loess at the pit was lost during the laboratory compaction. It has been tentatively confirmed by a single CIUP test on one saturated specimen which yielded the mobilised friction angle very close to φ_{cr} of the reconstituted specimens (Figure 6). In the figure, the suggested concept for the undrained strength of unsaturated soil (Figure 2) is demonstrated on just a simple pair of tests available to date (Table 3).

Table 3. Unconfined compression strength test vs CIUP triaxial test at an "identical" water content.

	w (%)	e	S_r (%)	σ_a' (kPa)	σ_r' (kPa)	s (kPa)
Unconfined compression strength	16.53	0.51	87.45	255.3	85.1	97.3
CIUP saturated	16.63	0.54	83.49	595	193	-

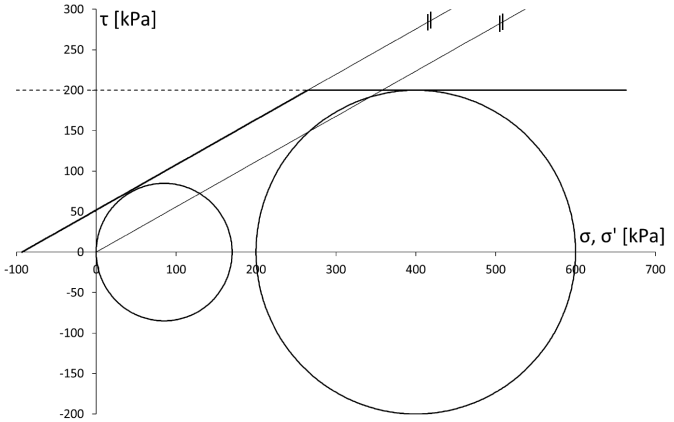

Figure 6. Mohr's circles - unsaturated unconfined compression test vs saturated CIUP triaxial test at an "identical" water content.

6.3 *Small strain stiffness*

In this section, the results of the drained shear probes in unsaturated conditions are presented. In addition, the maximum shear modulus for each net mean stress/suction stage was measured. The laboratory data are plotted together with the model interpretation – see Figure 7 and Figure 8.

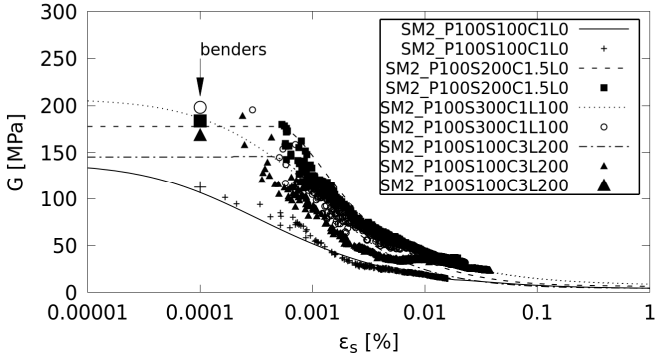

Figure 7. Stiffness degradation curves for different samples at p = 100kPa.

The stiffness is affected by the current suction, CSR, as well as the net mean stress. The results show very rapid decay of the stiffness. As Vucetic and Dobry (1991) or Coop et al. (1997) showed, the low plasticity soils have almost no maximum stiffness plateau. However, our results showed that the biggest part of stiffness degradation occurs in the region smaller than 0.001 % of shear strain. This phenomenon is then affecting the calibration of the hypoplastic model.

The measurements of the stiffness by the LVDTs are in good agreement with the maximum shear stiffness determined by the bender elements. Both LVDTs and bender elements measurements show an increase of the stiffness with the increasing suction. Also, the influence of CSR and recent suction history can be seen – e.g. SM2_P100S100C1L0 vs SM2_P100S100C3L200.

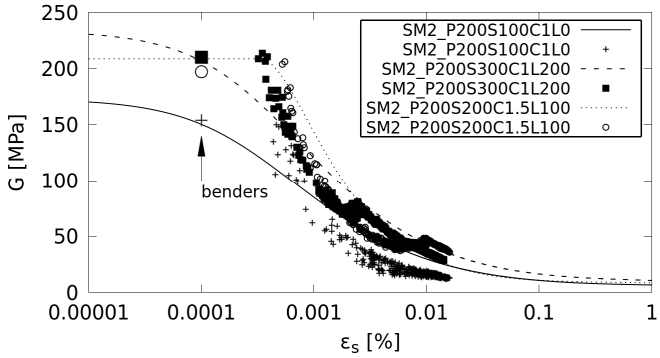

Figure 8. Stiffness degradation curves for different samples at p = 200kPa.

6.4 *Calibration*

The model was calibrated using the results from the saturated triaxial shear tests, saturated oedometric tests, bender element tests and LVDT measurements in unsaturated conditions. The model interpretation of the laboratory triaxial tests was done in a freeware element test constitutive model driver "Triax" (https://soilmodels.com/triax/). The parameters used in this study are summarized in Table 4. As mentioned in the section 6.3, the stiffness degradation is very rapid and occurs in the very small strain region. Thus, the size of the elastic range is shifted by the parameter *R* of the intergranular strain model.

Table 4. Soil parameters used for model calibration.

Basic model	φ_c	λ^*	κ^*	N	ν_{pp}	α_G
	30°	0.0706	0.0167	0.9470	0.25	1.0
Unsaturated mechanical model	n_s	l_s	m			
	0.0	0.0	1			
WRC model	s_{en0}	e_0	λ_{p0}	α_e		
	20	0.69	0.05	0.5		
Gtp0 model	A_g	n_g	m_g	k_g		
	6800	0.484	0.9	0.1		
Intergranular strain model	R	β_r	χ_g	m_{rat}	r_m	
	varies	1	1	1	0	

7 CONCLUSIONS

A simple way of determining the undrained strength s_u of an unsaturated silty clay for conventional undrained stability analyses has been presented. Both the used alternatives (SBS and hypoplastic model) comply with the concept of critical states.

The presented data of the ongoing experimental programme suggest that the simple approach is capable of yielding s_u for simple conventional analyses.

Advanced triaxial testing completed the set of parameters for the hypoplastic model, including the strain dependence of stiffness data, which will be used in verification of the simple analyses by FEM simulations of a case history of a clayey soil of variable saturation.

8 ACKNOWLEDGEMENTS

The financial support by the grant 17-21903S of the Czech Science Foundation (GAČR) and by the grant 1160217 of the Grant Agency of the Charles University (GAUK) is acknowledged.

9 REFERENCES

Bishop, A. W. 1959. The principle of effective stress. Tekniske Ukeblad, 39: 859-863.

Coop, M.R., Jovičić, V. & Atkinson, J.H. 1997. Comparisons between soil stiffness in laboratory tests using dynamic and continuous loading. *Proceedings of the Fourteenth International Conference on Soil Mechanics and Foundation Engineering* 1: 267-270.

Fredlund, D. G. & Morgenstern, N. R. 1977. Stress state variables for unsaturated soils. *Journal of Geotechnical Engineering* 103(5): 447-466.

Fredlund, D. G., Rahardjo, H. & Fredlund, M. D. 2012. Unsaturated soil mechanics in engineering practice. John Wiley & Sons.

Herle, I., Mašín, D., Kostkanová, V., Karcher, Ch. & Dahmen, D. 2011. Experimental investigation and theoretical modelling of soft soils from mining deposits. *Proceedings of the 5th International Symposium on Deformation Characteristics of Geomaterials* 2: 858-865.

Khalili N. & Khabbaz M.H. 1998. A unique relationship for the determination of the shear strength of unsaturated soils. *Géotechnique* 48(2): 1–7.

Lu, N. & Likos, W. J. 2004. Unsaturated soil mechanics. John Wiley & Sons.

Niemunis A. & Herle I. 1997. Hypoplastic model for cohesionless soils with elastic strain range. *Mechanics of Cohesive-frictional Materials* 2(4): 279-299.

Ng, C.W.W. & Xu, J. 2012. Effects of current suction ratio and recent suction history on small-strain behavior of an unsaturated soil. *Canadian Geotechnical Journal* 49(2): 226-243.

Schofield, A.N. & Wroth, C.P. 1968. Critical state soil mechanics. McGraw Hill, Maidenhead.

Sharma, B. and Bora, P. K. 2003. Plastic limit, liquid limit and undrained shear strength of soil - reappraisal. *Journal of Geotechnical and Geoenvironmental Engineering*, 129(8): 774–777.

Vucetic, M. & Dobry, R. 1991. Effect of Soil Plasticity on Cyclic Response. *Journal of Geotechnical Engineering* 117(1): 89-107.

Wong, K.S., Mašín, D. 2014. Coupled hydro-mechanical model for partially saturated soils predicting small strain stiffness. *Computers and Geotechnics* 61: 355-369.

HYPERLINK
"https://soilmodels.com/triax/"